Electronic Supplementary Material (ESI) for Journal of Materials Chemistry A.

Supplementary Information

An adaptive supramolecular organic framework for highly efficient separation of uranium via in situ induced fit mechanism

Bo Li, Chiyao Bai, Shuang Zhang, Xiaosheng Zhao, Yang Li, Lei Wang, Kuan Ding, Xi Shu, Shoujian Li* and Lijian Ma*

College of Chemistry, Sichuan University, Key Laboratory of Radiation Physics & Technology (Sichuan University), Ministry of Education, Chengdu 610064, P. R. China.

*Corresponding author.

Tel.: +86 28 85412329

Fax: +86 28 85412907

E-mail address: sjli000616@scu.edu.cn (S. Li).

Section 1. Preparation of U(VI) stock solution, La(III) test solution and multi-ion solution

The stock solution of uranyl nitrate (~1000 mg L^{-1}) or lanthanum nitrate (~1000 mg L^{-1}) were prepared by dissolving appropriate amounts of $UO_2(NO_3)_2 \cdot 6H_2O$ or $La(NO_3)_3 \cdot 6H_2O$ in deionized water. Then working solution (100–300 mg L^{-1}) was prepared by diluting the stock solution with deionized water to demanded concentrations, and adjusted to desired pH value using a negligible volume of dilute solution of sodium hydroxide and/or nitric acid when needed. Similarly, the multi-ion solution containing 11 competing ions besides U(VI) as listed in Table S4, was prepared by dissolving the metal oxides or nitrates in nitric acid aqueous solution with the each metal concentration of about 1.00 mmol L^{-1}.

Section 2. High resolution XPS spectra of C 1s.

For the C 1s XPS spectra of MA-TMA shown in Fig. S5, the binding energies at 284.5 eV belong to sp^2 hybridized carbon, 285.4 eV to C=N, 286.3 eV to C–O or C–N and 288.3 eV to C=O.[1,2]

Table S1. Operating parameters for ICP-AES

Radio-frequency (RF) power (W)	1150
Carrier argon flow rate (L min^{-1})	0.6
Auxiliary argon flow rate (L min^{-1})	Low
Coolant argon flow rate (min^{-1})	14
Nebulizer gas (PSI)	27
Integration time (s)	25
Wavelength (nm)	U 385.9； Gd 342.2 Sm 442.4； Nd 430.4 La 333.7； Ce 413.3 Ni 231.6；Zn 213.8 Co 228.6；Ba 493.4 Sr 407.7；Mn 257.6

Table S2. Different experimental conditions for the preparation of the MA-TMA and it's adsorption capacity and selectivity (S_U) toward uranium [a]

Number	Molar ratio	Dropping rate (mL min^{-1})	T (K)	t (h)	q_{tol} (mmol g^{-1})	q_e (mmol g^{-1})	S_U (%)
1	1：1	120	333	2	2.66	1.01	38.0
2	1：1	60	353	4	2.69	1.04	38.7
3	1：1	30	373	6	2.78	1.05	37.6
4	5：1	60	333	6	2.12	1.04	48.9
5	5：1	30	353	2	1.99	1.06	53.0
6	5：1	120	373	4	2.11	0.966	45.9
7	1：5	30	333	4	2.80	1.05	37.6
8	1：5	120	353	6	2.77	1.02	36.8
9	1：5	60	373	2	2.85	1.03	36.0

[a]. Sorption conditions: $C_o \approx 0.45$ mmol L^{-1} for U(VI) and 0.5 mmol L^{-1} for other cations, pH = 4.5, t = 120 min, V = 25 mL, T = 298 K, and ω = 10 mg.

Table S3. Different molar ratio for the preparation of the MA-TMA and it's adsorption capacity and selectivity (S_U) toward uranium[a]

Number	Molar ratio	T (K)	Dropping rate (mL min^{-1})	t (h)	q_{tol} (mmol g^{-1})	q_e (mmol g^{-1})	S_U (%)
1	5：1	353	30	2	1.84	1.12	61.2
2	25：5	353	30	2	1.82	1.11	61.1
3	10：1	353	30	2	1.82	1.09	60.4

[a]. Sorption conditions: $C_o \approx 0.47$ mmol L^{-1} for U(VI) and 0.5 mmol L^{-1} for other cations, pH = 4.5, t = 120 min, V = 25 mL, T = 298 K, and ω = 10 mg.

Table S4. Compositions of the simulated nuclear industrial effluent

Coexistent ion	Added as	Reagent purity
UO_2^{2+}	$UO_2(NO_3)_2 \cdot 6H_2O$	Standard reagent
La^{3+}	$La(NO_3)_3 \cdot 6H_2O$	99.9% metal basis
Ce^{3+}	$Ce(NO_3)_3 \cdot 6H_2O$	99.99% metal basis
Nd^{3+}	$Nd(NO_3)_3 \cdot 6H_2O$	AR
Sm^{3+}	$Sm(NO_3)_3 \cdot 6H_2O$	AR
Gd^{3+}	$Gd(NO_3)_3 \cdot 6H_2O$	AR
Mn^{2+}	MnO	99.5%
Co^{2+}	$Co(NO_3)_2 \cdot 6H_2O$	99.99% metal basis
Ni^{2+}	$Ni(NO_3)_2 \cdot 6H_2O$	Spectrum pure
Zn^{2+}	$Zn(NO_3)_2 \cdot 6H_2O$	99.99% metal basis
Sr^{2+}	$Sr(NO_3)_2$	99.99% metal basis
Ba^{2+}	$Ba(NO_3)_2$	99.999%

Table S5. Kinetic parameters for the U(VI) adsorption onto MA-TMA

q_e (exp)	pseudo-first-order equation			pseudo-second-order equation		
(mg g^{-1})	$q_{e,cal}$ (mg g^{-1})	k_1 (min^{-1})	R^2	$q_{e,cal}$ (mg g^{-1})	k_2 (g mg^{-1} min^{-1})	R^2
259.7	130.8	0.4246	0.9939	269.5	0.006588	0.9999

Intrapaticle diffusion		
k_{int} (mg g^{-1} $min^{-(1/2)}$)	C mg g^{-1}	R^2
46.96	133.2	0.8489

Table S6. Thermodynamic parameters for the U(VI) adsorption onto MA-TMA

ΔH (kJ mol^{-1})	ΔS (J mol^{-1} K^{-1})	ΔG (kJ mol^{-1})				
		298	308	318	328	338
-14.62	0.5068	-14.77	-14.78	-14.78	-14.79	-14.79

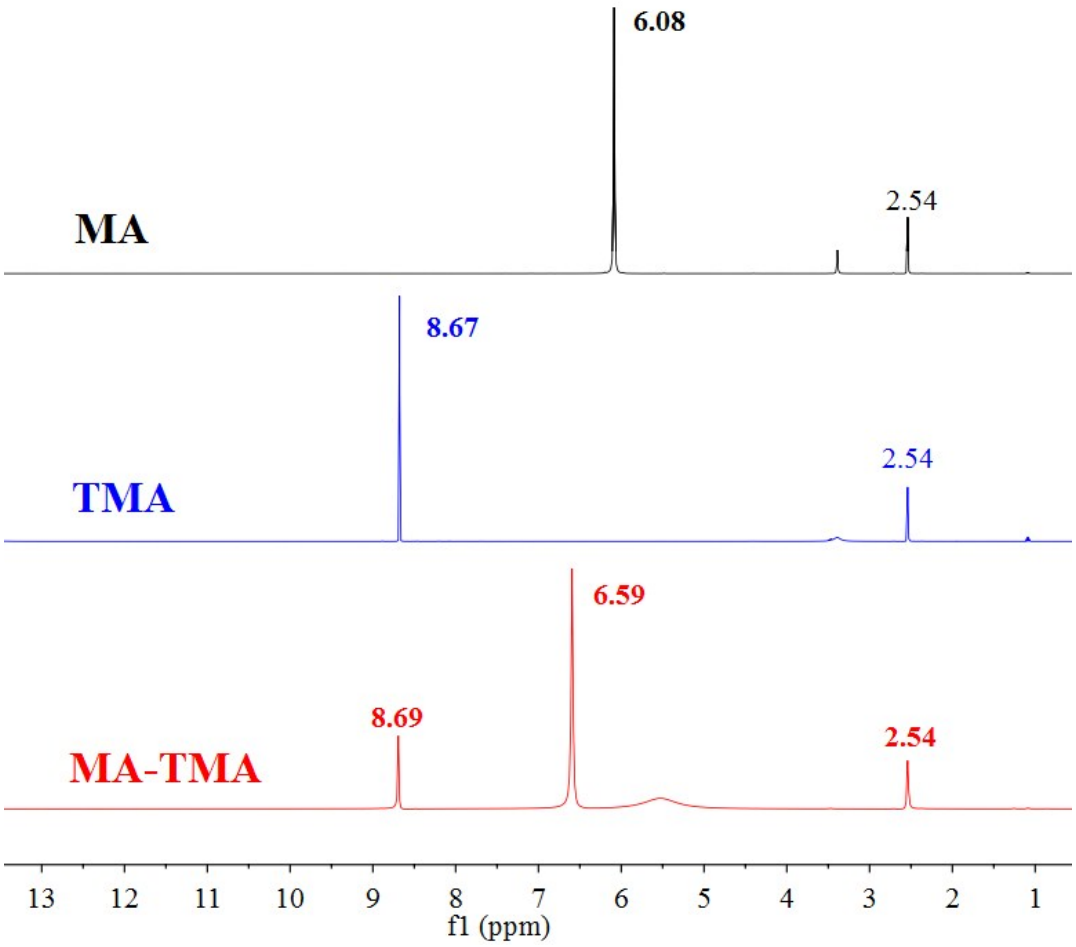

Fig. S1 ^{1}H NMR signal of MA,TMA and MA-TMA in DMSO.

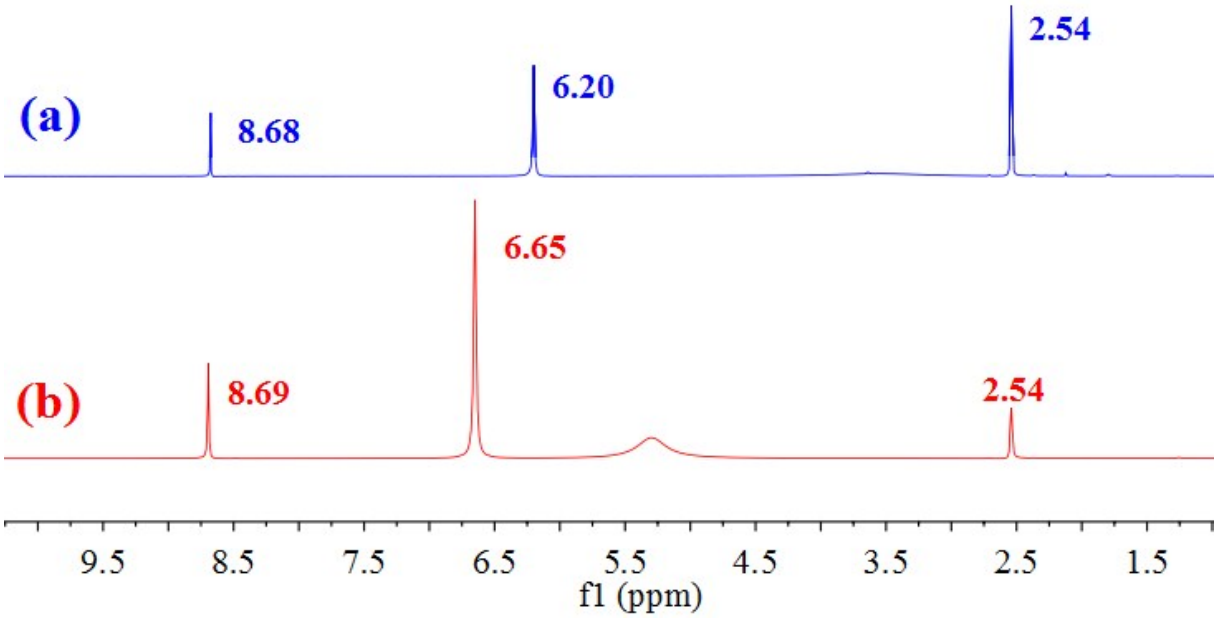

Fig. S2 ^{1}H NMR signal of MA-TMA at different concentration in DMSO. (a) 5 mg of MA-TMA dissolved in DMSO at a concentration of 10 mg mL^{-1}, (b) 15 mg of MA-TMA dissolved in DMSO at a concentration of 30 mg mL^{-1}.

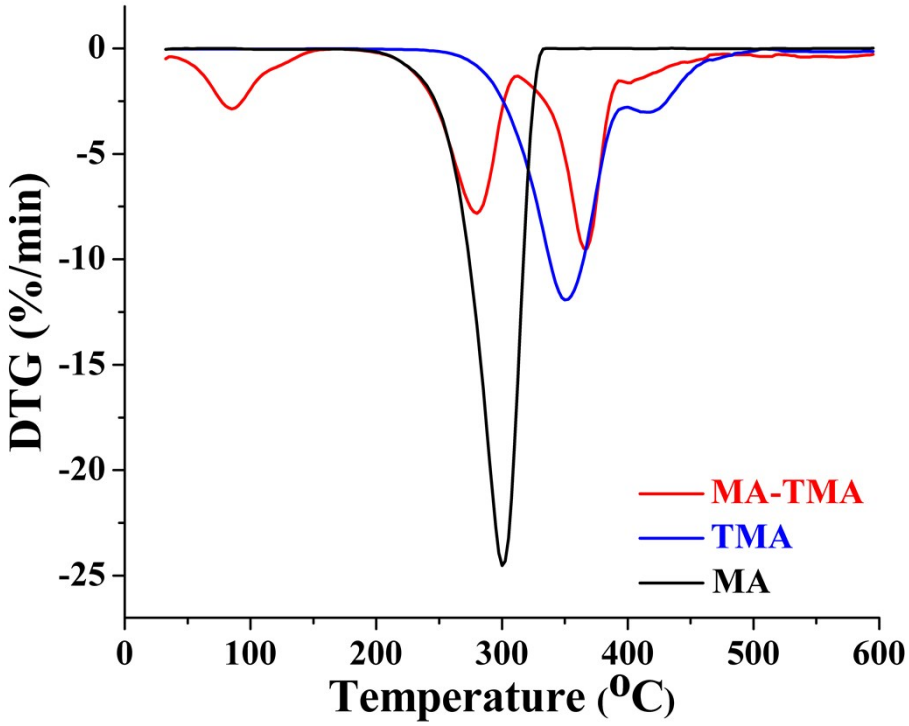

Fig. S3 DTG analysis of MA, TMA, and MA-TMA.

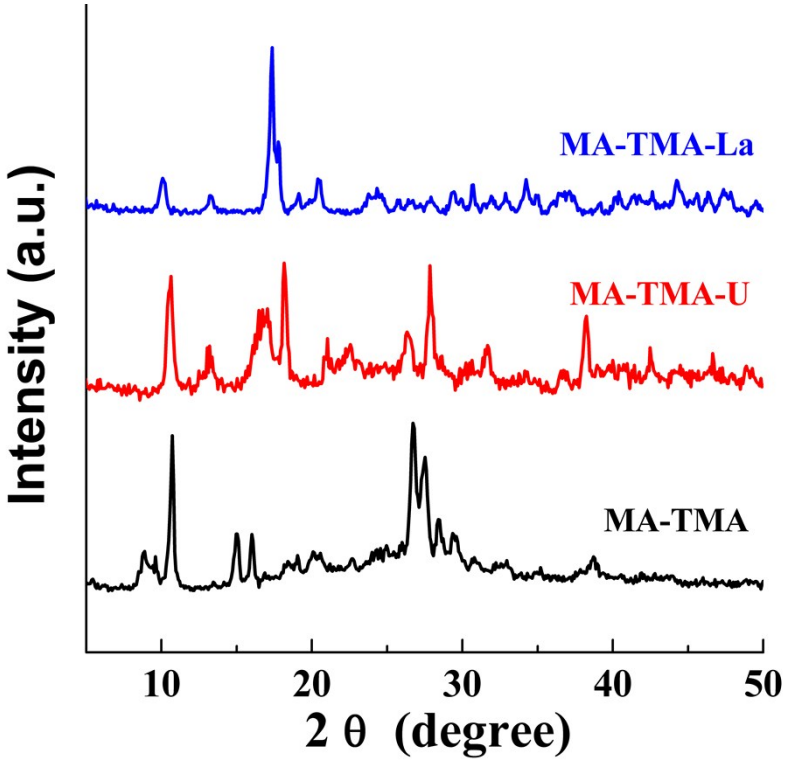

Fig. S4 Powder X-ray diffraction spectra of MA-TMA and MA-TMA-U and MA-TMA-La.

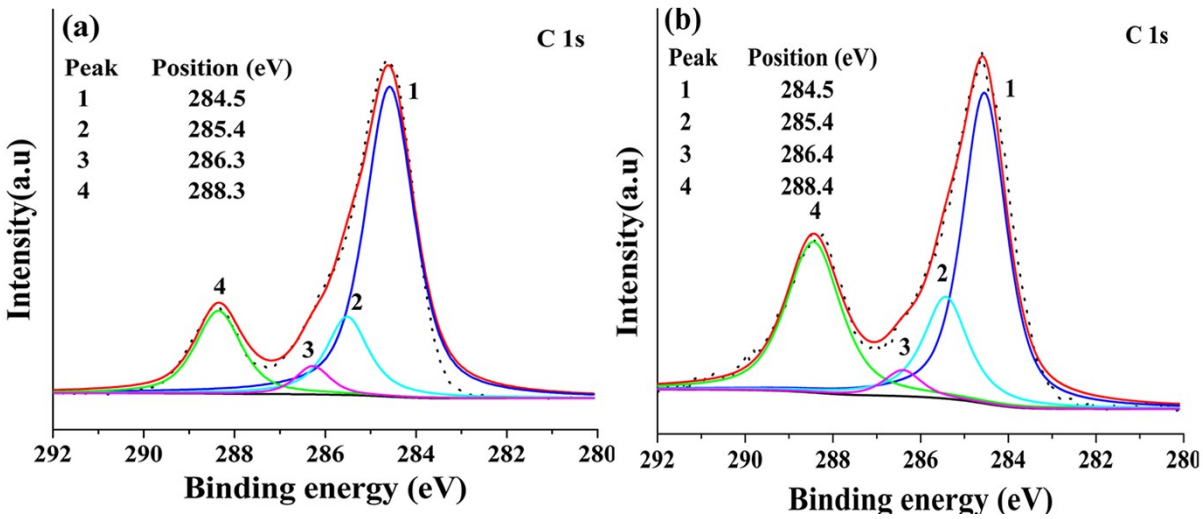

Fig. S5 High resolution XPS spectra of C1s for (a) MA-TMA and (b) MA-TMA-U.

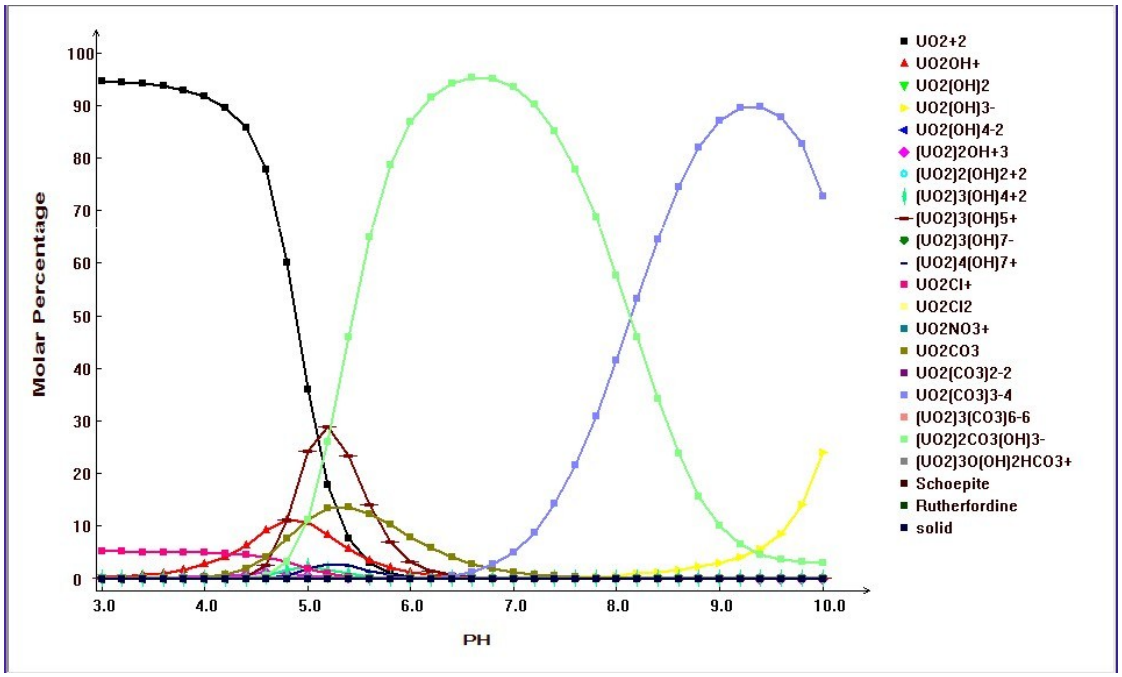

Fig. S6 Distribution of U(VI) species in aqueous solution with a total concentration of 300 mg L^{-1} and pH values ranging from 3 to 10. Calculated by using a CHEMSPEC (C++) program.

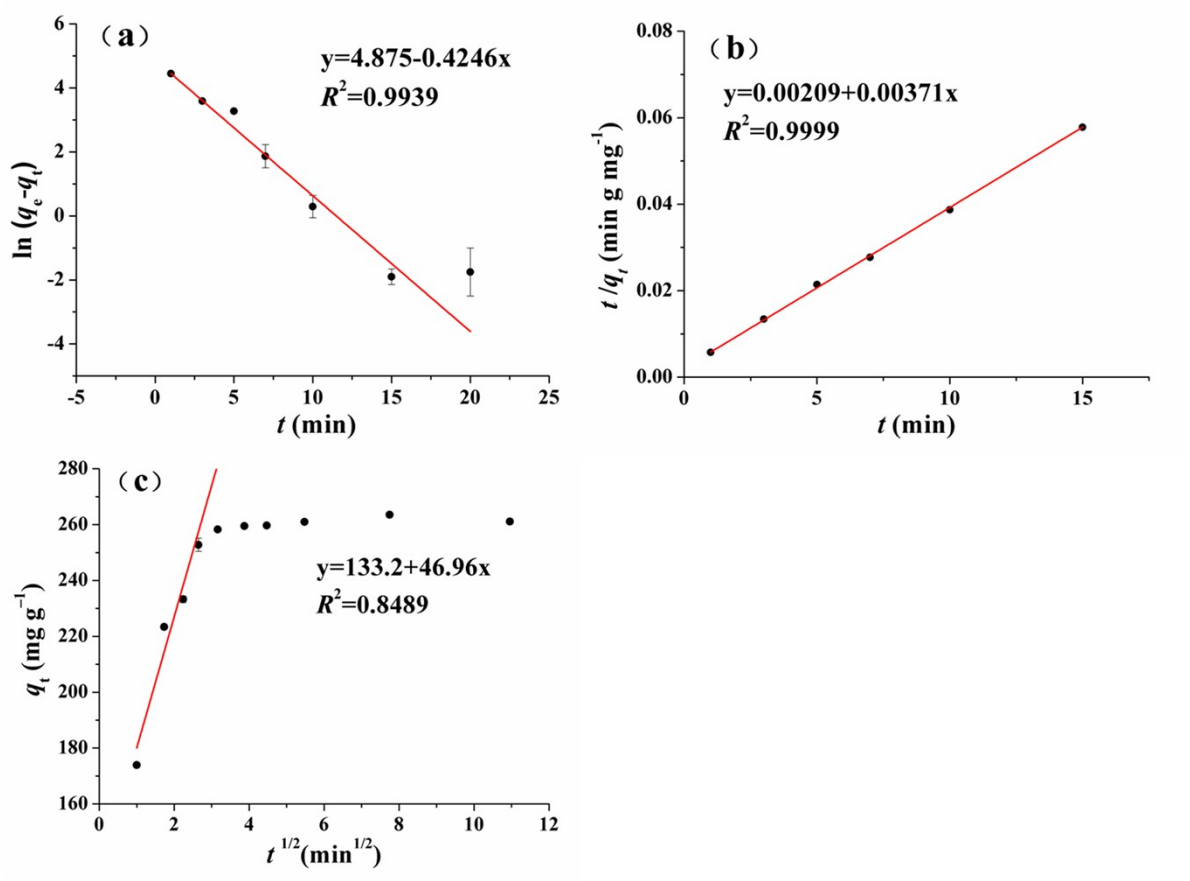

Fig. S7 (a) Pseudo-first-order, (b) pseudo-second-order and (c) intraparticle diffusion model plots for the adsorption of U(VI) onto MA-TMA.

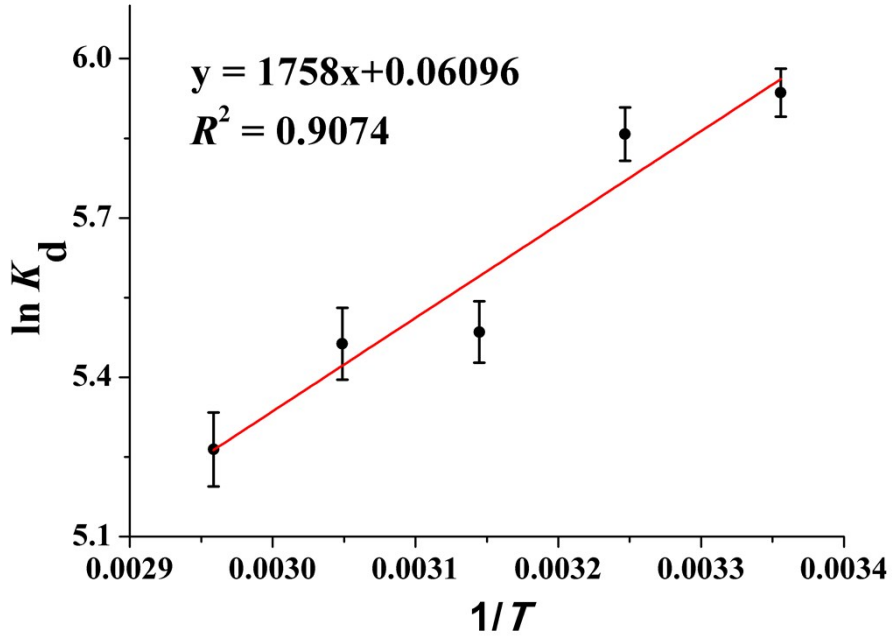

Fig. S8 Plot of ln Kd vs. 1/T for the adsorption of U(VI) onto MA-TMA ($C_o \approx 100$ mg L^{-1}, pH = 4.5, t = 120 min, V = 25 mL, and ω = 10 mg).

Reference

1 Z. X. Chen , Q. F. Zhang, L. Huang, R. Li, W. C. Li, G. Q. Xu, and H. S. Cheng, *J. Phys. Chem. C,* 2014, **118**, 21244.

2 S. Y. Jeong, S. H. Kim, J. T. Han, H. J. Jeong, S. Yang and G.-W. Lee, *Acs Nano*, 2011, **5**, 870.